

WIDTH-PULSE CONTROL OF A FLEXIBLE SATELLITE AT DAMPING AND GUIDANCE ON THE SUN AND THE EARTH

Sergey Somov

Department " Dynamics and Motion Control "
Samara Scientific Center, Russian Academy of Sciences (RAS)
Russia
s.somov@mail.ru

Abstract

Problems of nonlinear modeling, dynamic analysis, simulation of spatial motion by a spacecraft with a flexible weak damping structure, are considered. The obtained results on a multi-rate filtering measurements and a width-pulse modulation of the jet engine thrust control, simulation and animation for the communication satellite with large-scale solar array panels by the *Sesat* type at modes of initial damping and guidance on the Sun and on the Earth, are represented.

Key words

Control of oscillations, motion control, applications

1 Introduction

For large-scale spacecraft (SC) the structure oscillations can render an essential influence on its spatial motion, it is especially for an initial mode after separation from a launcher, and also at the SC initial guidance on the Sun and on the Earth. Modern computer technology allows to obtain a dynamic analysis and a video-display the SC structure deformations during its spatial motion. That it is very useful at a SC designing and flight support. The SC *Sesat* (fig. 1) with large-scale



Figure 1. The satellite *Sesat*.

flexible solar array panels (SAPs) was developed by *Reshetnev NPO PM* (Russia) under the contract with *Eutelsat* and was removed on geostationary orbit in April 2000. In the paper for this type SC the spatial motion models are created at a width-pulse modulation (WPM) of control by jet engines and the SAPs' bend-

turning oscillations, results on a control laws' synthesis for the initial modes, simulation and animation both the SC body and the SAPs motion, are presented.

2 Modeling a satellite structure motion

A lot of publications were devoted for a choice of dynamic schemes, methods for deriving and research the flexible SC motion equations, analytical reviews are well-known, but the problem of development the effective methods for modeling dynamics and imitation of the SC motion is remained actual. At deriving the approximate models of the flexible SC motion the Reley-Ritz-Galerkin method – the method of the prospective oscillation forms, is most known. At synthesis of the SC dynamic models with non-rigid structure the method of fixed elements (MFE) is widely applied. The MFE represents a located method of prospective oscillation forms.

Having doubtless advantages and advanced software (NASTRAN, ASKA, SAP-IV etc.), the MFE generates models with rather high dimension reaching several thousand on degrees of freedom for complex ramified spacecraft structures.

Peculiarity of the applied approach consists in presentation of the structure elements' flexible oscillations by fixed number of tones. Here calculation is carried out by the MFE with condensation (reduction) on the oscillation tones, the factor matrixes of interference for motions of all sub-structure both rigid and deformable bodies, are also calculated by computer. Own forms and own partial frequencies of flexible oscillations by each SAP for the SC *Sesat* was carried out taking into account $n^q = 10$ lowest tones in standard normalization, fig. 2. Design scheme of the SAPs' first wing for spacecraft *Sesat* is represented in fig. 3) by the fixed-element model consisting 129 main points where 33 points are the concentrated weights, and 205 beams with five various geometrical and two various physical properties (Butyrin and Somov, 2004).

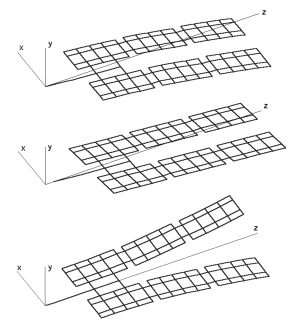


Figure 2. The lowest tones

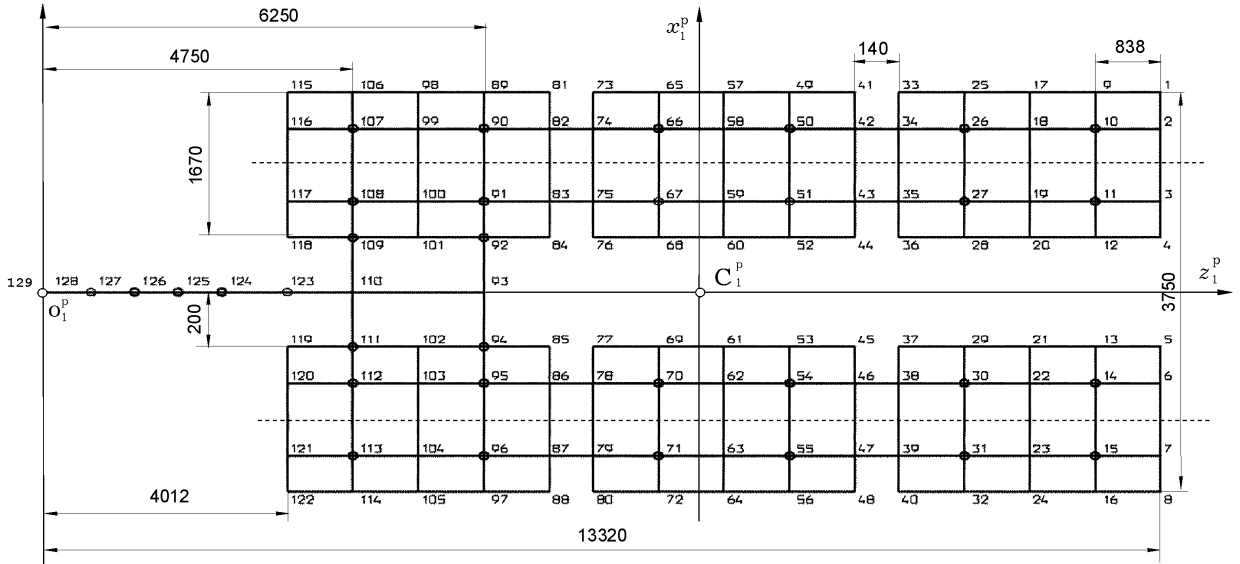


Figure 3. The design scheme for the SAPs' first wing of spacecraft Sesat by method of fixed elements.

The model of the angular motion dynamics by the spacecraft with active flexible SAPs was elaborated at assumptions

- position of the mass center for all mechanical system have small differ from nominal position – a pole O at derivation of nonlinear equations for system spatial motion;
- the SAPs move according to command rate as piece-constant time function that is caused by step-by-step gear driver (SGD) with self-braking.

That model have the form

$$\mathbf{A}^o \begin{bmatrix} \dot{\boldsymbol{\omega}} \\ \ddot{\mathbf{q}} \end{bmatrix} = \begin{bmatrix} \mathbf{F}^\omega \\ \mathbf{F}^q \end{bmatrix}; \mathbf{A}^o = \begin{bmatrix} \mathbf{J}(\gamma) & \mathbf{D}^q(\gamma) \\ (\mathbf{D}^q(\gamma))^t & \mathbf{I}_{2n^q} \end{bmatrix}; \quad (1)$$

$$\mathbf{F}^\omega \equiv -\boldsymbol{\omega} \times \mathbf{G} + \mathbf{M}_o^{\text{do}} + \mathbf{M}_o^p + \mathbf{M}_o;$$

$$\mathbf{F}^q \equiv -(\mathbf{D} \dot{\mathbf{q}} + \mathbf{W} \mathbf{q} + (\mathbf{D}_3^q(\gamma))^t \ddot{\gamma}).$$

Here $\boldsymbol{\omega} = \{\omega_x, \omega_y, \omega_z\}$ is a vector of the SC angular rate in the body reference frame (BRF) $Oxyz$, the inertia tensor $\mathbf{J} = \mathbf{J}(\gamma) = \mathbf{J}^o + 2\mathbf{J}^p(\gamma)$ at any position of the SAPs, determined by a angle γ , and the inertia tensor for each wing of the SAPs is as follows:

$$\mathbf{J}^p(\gamma) = \begin{bmatrix} J_x^p C_\gamma^2 + J_y^p S_\gamma^2 & J_{xy}^p C_\gamma S_\gamma & 0 \\ J_{xy}^p C_\gamma S_\gamma & J_x^p S_\gamma^2 + J_y^p C_\gamma^2 & 0 \\ 0 & 0 & J_z^p \end{bmatrix},$$

where $J_{xy}^{\text{pd}} = J_x^p - J_y^p$ and $C_\gamma = \cos \gamma; S_\gamma = \sin \gamma$. Rectangular matrix $\mathbf{D}^q(\gamma)$ of an inertial influence by the SAPs and the SC body motions is represented by matrix-line $\mathbf{D}^q = [\mathbf{D}_1^q, \mathbf{D}_2^q]$, and the structure of matrixes \mathbf{D}_1^q and \mathbf{D}_2^q by flexible SAPs inertial influence is those: the matrix $\mathbf{D}_k^q = \{\mathbf{D}_{k1}^q, \mathbf{D}_{k2}^q, \mathbf{D}_{k3}^q\}$ is represented by column, where \mathbf{D}_{kj}^q is line. Here $j = 1, 2, 3$

is the line number and $k = 1, 2$ is the wing number. Then, $\mathbf{G} = \mathbf{J}(\gamma) \boldsymbol{\omega} + \mathbf{H} + \mathbf{D}^q(\gamma) \dot{\mathbf{q}}$ is vector of the flexible SC angular momentum where \mathbf{H} is vector of the gyro stabilizer's own momentum and the torque vector

$$\mathbf{M}_o^p = \begin{bmatrix} (J_{xy}^{\text{pd}}(S_{2\gamma}\omega_x - C_{2\gamma}\omega_y) - 2J_z^p\omega_y) \dot{\gamma} \\ -(J_{xy}^{\text{pd}}(C_{2\gamma}\omega_x - S_{2\gamma}\omega_y) + 2J_z^p\omega_y) \dot{\gamma} \\ -2J_z^p \ddot{\gamma} \end{bmatrix}$$

presents the inertial-gyroscopic forces, caused by the SAPs activity. Vector $\mathbf{q} = \{\mathbf{q}_1, \mathbf{q}_2\}$ presents the generalized coordinates of the SAPs flexible oscillations, $\mathbf{q}_k \in \mathbf{R}^{n^q}$ is vector of the same coordinates by k -th wing. Diagonal matrix $\boldsymbol{\Omega}_k = \text{diag}\{\Omega_{ks}\}$ is made from partial frequencies Ω_{ks} , $s = 1 : n^q$ and δ is logarithmic decrement of the SAPs' oscillations, matrixes $\boldsymbol{\Omega} = \text{diag}\{\boldsymbol{\Omega}_1, \boldsymbol{\Omega}_2\}$, $\mathbf{D} = (\delta/\pi)\boldsymbol{\Omega}$, $\mathbf{W} = \boldsymbol{\Omega}^2$, $\mathbf{D}_3^q = \{\mathbf{D}_{13}^q, \mathbf{D}_{23}^q\}$. Vector $\mathbf{M}_o = \mathbf{M}_o^g + \mathbf{M}_o^s$ presents external torques with respect to a pole O , where \mathbf{M}_o^g is a vector of gravitational torque and \mathbf{M}_o^s – a torque vector by forces of solar pressure. At last, vector \mathbf{M}_o^{do} presents the orientation engine unit (OEU) torques.

The motion model of the SC body with active SAPs is easily turned out from (1) and have the form

$$\mathbf{J} \dot{\boldsymbol{\omega}} + \boldsymbol{\omega} \times \mathbf{J} \boldsymbol{\omega} = \mathbf{F}^\omega \equiv \mathbf{M}_o^{\text{do}} + \mathbf{M}_o^p + \mathbf{M}_o. \quad (2)$$

The BRF orientation with respect to orbital reference frame (ORF) $O x^o y^o z^o$ is defined by quaternion $\boldsymbol{\Lambda}^o$ according to the differential equation

$$\dot{\boldsymbol{\Lambda}}^o = \frac{1}{2} (\boldsymbol{\Lambda}^o \circ \boldsymbol{\omega} - \dot{\nu}_o^o \circ \boldsymbol{\Lambda}^o), \quad (3)$$

where vector-column $\dot{\nu}_o^o(t) = \{0, 0, \dot{\nu}_o(t)\}$ represents a vector $\dot{\nu}_o(t)$ of the SC orbital angular rate in projections on the ORF axes and $\nu_o(t)$ is true orbital anomaly.

The SC orbit is considered known, direction of unit \mathbf{E} on the Earth is also known, thus the vector of gravitational torque \mathbf{M}_o is represented by analytical dependence only from quaternion Λ^o of the SC orientation with respect to the ORF.

The BRF attitude with respect to the inertial reference frame (IRF) is defined by quaternion Λ according to the differential equation $\dot{\Lambda} = \Lambda \circ \omega / 2$. Therefore direction of unit \mathbf{S} on the Sun is also known and a torque vector \mathbf{M}_o^s by forces of solar pressure is represented by analytical relations.

3 Models of the control system's components

The instrument set of the SC attitude control system (ACS) in the initial damping mode consists the OEU based on six thermo-catalytic jet engines (JEs) with the thrust WPM, a block of three one-axial angular rate sensors (ARSs), the SGD and an angular position sensor by two SAPs' wings with respect to the SC body, and also on-board computer. At mode of the SC guidance on the Sun in the ACS instrument composition is completed by the Sun sensor (SS) with wide segmented field-of-view (fig. 4) and at mode of the SC guidance on the Earth — by the Earth sensor (ES) with narrow field-of-view, fig. 5. Standard denotations for values of a scalar discrete signal $y(t_k) = y_k$ and $y(t_s) = y_s$ are further applied at the time moments $t_k = k T_u$ with the control period T_u and multiple by their the time moments $t_s = s T_q$ with the measurement period T_q where integers $k, s \in \mathbb{N}_0 \equiv [0, 1, 2, \dots]$, moreover the multiple index $n_q = T_u / T_s$.

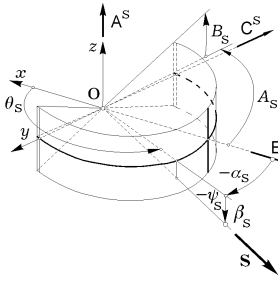


Figure 4. The SS scheme.

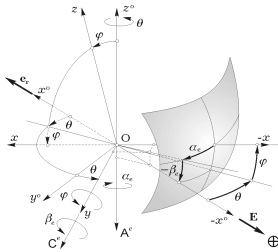


Figure 5. The ES scheme.

3.1 The OEU model

For the WPM of normalized command by the thrust inclusion $P^n(t, \tau_k^d) \in \{0, 1\}$, $k \in \mathbb{N}_0$ by each JE, namely $P^n(t, \tau_k^d) = 1 \forall t \in [t_k, t_k + \tau_k^d)$ and $P^n(t, \tau_k^d) = 0 \forall t \in [t_k + \tau_k^d, t_{k+1})$ the modulation characteristic is described by the ratio $\tau_k^d = \varphi^d(\tau_m, \tau^m, T_u, \tau_k)$:

$$\tau_k^d = \begin{cases} 0 & \tau_k < \tau_m; \\ \tau_k & \tau_m \leq \tau_k < \tau^m; \\ \tau^m & \tau^m \leq \tau_k < T_u; \\ T_u & \tau_k > T_u. \end{cases} \quad (4)$$

Taking into account a time (transport) delay T_{zu}^d dynamic processes on the normalized thrust $P_d^n(t)$ for each JE are presented by the differential equation $T^d \dot{P}_d^n + P_d^n = P^n(t - T_{zu}^d, \tau_k^d)$ with the initial condition $P_d^n(t_0) = 0$ where a time constant T^d accepts two values T_+^d or T_-^d according to the ratio: *if* $P^n = 1$ *then* $T^d = T_+^d$ *else* $T^d = T_-^d$. For everyone j -th JE D_j , $j = 1 : 6$ there is compared the vector $\mathbf{P}_j(t) = P^m P_d^n(t) \mathbf{p}_j$ of the current jet thrust with fixed unit \mathbf{p}_j beginning in a point O_j^d where P^m is the current maximal thrust value, identical for all JEs. The point O_j^d arrangement is defined by a radius-vector ρ_j . The OEU control torques concerning axes Ox , Oy and Oz are created by JEs' pairs. Logic of the command τ_{jk} formation for inclusion everyone j -th JE takes into account a sign of a command signal v_{ik} on channel $i = x, y, z$ and is described by such algorithm: $\tau_{ik} = |v_{ik}|$; $s_{ik} = \text{sign } v_{ik}$; $i = x, y, z$ and then, for example for $i = x$: *if* $s_{xk} > 0$ *then* ($\tau_{1k} = \tau_{xk} \& \tau_{2k} = 0$) *else* ($\tau_{1k} = 0 \& \tau_{2k} = \tau_{xk}$). Formed by the OEU the control torque vector \mathbf{M}_o^{do} is calculated by formula

$$\mathbf{M}_o^{\text{do}} \equiv \mathbf{M} = \{M_x, M_y, M_z\} = \sum_{j=1}^6 \rho_j^d \times \mathbf{P}_j. \quad (5)$$

3.2 Model of the SC body rate measurement

The model of the ARS block for measuring the SC body rate vector represents by set of three same channels for measurement $\omega_i(t)$, $i = x, y, z$, moreover model of each its channel takes into account: own dynamical properties; a noise and systematic errors; a time sampling, quantization and limit levels. Description of the measurement process for a projection of angular rate $\omega(t)$ is presented as follows:

$$\begin{aligned} T^\omega \dot{\omega}^s(t) + \omega^s(t) &= \omega(t); \\ \omega^{\text{se}}(t) &= \text{Sats}(a^\omega, k^\omega, \omega^s(t) + b^\omega); \\ \omega_s^\sigma &= \omega^{\text{se}}(t_s) + \omega_s^n; \omega_s^d = \text{Qntr}(d^\omega, \omega_s^\sigma). \end{aligned} \quad (6)$$

Here T_q is a time sampling period and T^ω is a time constant; a^ω and k^ω are a restriction level and the normalized gain; there are applied the standard functions $y = \text{Sats}(a, k, x)$: *if* $|x| \leq a/k$ *then* $y = k x$ *else* $y = a \text{sign } x$ and $y = \text{Qntr}(d, x) = d \text{E}[(x/d) + 0.5 \text{sign } x]$ where d is a quantization step and $\text{E}[\cdot]$ is a symbol of the whole part for number $[\cdot]$; b^ω is slowly varied "zero drift"; ω_s^n is discrete noise of measurement which is considered as Gauss stochastic discrete process with a zero mean and root-mean-square deviation σ^ω ; d^ω is a quantization step by an output signal, at last ω_s^d is a discrete output signal.

3.3 Models of the Sun and the Earth sensors

The SS outputs are a sign N^s of the Sun presence into its field-of-view and the spherical angular coordinates θ_s, ψ_s of unit \mathbf{S} with respect to the BRF Ox axis, see

fig. 4. The SS digital output signals $\theta_{S_s}^d$ and $\psi_{S_s}^d$ then are filtering by a computer processing. The ES outputs are a sign N^e of the Earth presence into its field-of-view and digital values of pitch angle θ_s^d and roll angle φ_s^d , see fig. 5.

3.4 Model of control contour at the SAPs guidance

The control contour by the SAPs position sensor and the GSD is presented by set of a discrete subsystem with forming error $\varepsilon_k^\gamma = \gamma_k^c - \text{Qntr}(d^\gamma, \gamma_k)$ and a piecewise-continuous part $\dot{\gamma}(t) = \text{Zh}(T_u, \dot{\gamma}_k^d)$ with initial condition $\gamma(t_0) = \gamma_0$. Here γ_k^c is a discrete command signal, $\dot{\gamma}_k^d = k^\gamma \varepsilon_k^\gamma$ and the holder with period T_u is such: $y(t) = \text{Zh}[T_u, x_k] = x_k \forall t \in [t_k, t_{k+1})$.

4 Algorithms of discrete filtering and control

Operator for averaging with identical weights only n_q last measurements y_s of a signal with obtaining an estimation \bar{y}_k , optimum on method of the least squares, have the description

$$\bar{y}_k = \text{MS}(y_s) \equiv \left(\sum_{s=k-n_q+1}^k y_s \right) / n_q; k = E[s/n_q].$$

For example, for SC Sesat it is accepted $T_q = 1$ s and $T_u = 4$ s, therefore the multiple index $n_q = 4$. That operator is applied for multiple filtering the discrete output signals $\omega_{i_s}^d$ of the ARSs on channels ($i = x, y, z$) and the discrete output signals of the SS and the ES:

$$\begin{aligned} \bar{\omega}_{i_k} &= \text{MS}(\omega_{i_s}^d); \\ \bar{\theta}_{S_k} &= \text{MS}(\theta_{S_s}^d); \quad \bar{\psi}_{S_k} = \text{MS}(\psi_{S_s}^d); \\ \bar{\varphi}_k &= \text{MS}(\varphi_s^d); \quad \bar{\theta}_k = \text{MS}(\theta_s^d). \end{aligned} \quad (7)$$

At initial damping mode, forming the discrete command signals v_{ik} on channels is defined as follows:

$$v_{ik} = k_i^\omega (\omega_i^c - \bar{\omega}_{i_k}), \quad i = x, y, z. \quad (8)$$

Here k_i^ω are the gain factors which are formed by relations $k_i^\omega = k_p c_i^\omega$; $k_p = P_f^m / P^m$, where k_p is the adjusted parameter for compensation of the JE's thrust variation; c_i^ω — values of the gain factors at a minimum level P_f^m of the JE's thrust.

For guidance the SC on the Sun by shortest way after its appearing into the SS field-of-view (e.g. at $N^s = 1$) the discrete vector control algorithm is suggested. Let us a constant vector \mathbf{b}^s for required position of the unit \mathbf{S} in the BRF and vector $\mathbf{p}_k = \{p_{1k}, p_{2k}, p_{3k}\}$ is computed by relation $\mathbf{p}_k = \mathbf{b}^s \times \bar{\mathbf{S}}_k(\bar{\theta}_{S_k}, \bar{\psi}_{S_k})$. According to elaborated algorithm there is forming a preliminary discrete signal $\tilde{v}_{ik} = -k_p (k_i^p p_{ik} + k_i^\omega \bar{\omega}_{i_k})$, $i = x, y, z$. Than value $\tilde{v}_{ik}^m = \max(|\tilde{v}_{ik}|, i = x, y, z)$ is computed and at condition $\tilde{v}_{ik}^m > T_u$ the resulting discrete controls on channels are scaling by simple formula $v_{ik} = T_u \tilde{v}_{ik} / \tilde{v}_{ik}^m$, $i = x, y, z$.

5 Dynamical properties of flexible spacecraft

Both linear and nonlinear methods were applied for dynamical research of the robust SC ACS with a width-pulse modulation of the jet engine thrust control.

After separating a SC from buster and disclosing the SAPs at any time moment $t = t_0$ the angular rate vector accepts a value $\omega(t_0) \in \mathbf{S}_\omega$ from the bounded convex domain \mathbf{S}_ω . Let the constant command values ω_i^c (components of the command angular rate vector ω^c) are given and them should be reached with given accuracy $|\omega_i(t) - \omega_i^c| \leq \delta_\omega \forall t \geq t_0 + T_r$ for some acceptable duration T_r of damping mode. For spacecraft by Sesat type at this mode additional requirement consists in a simultaneous turning the SAPs on the angle $3\pi/2$ with respect to the SC body. In this mode at any SAPs fixed position and the gyro stabilizer momentum $\mathbf{H} = \mathbf{0}$, linearized in the IRF the continuous model of free flexible SC controlled motion have the form

$$\mathbf{A}_1 \{\dot{\omega}, \ddot{\mathbf{q}}, \dot{\mathbf{q}}\} = \mathbf{B}_1 \{\delta\omega, \dot{\mathbf{q}}, \mathbf{q}\} + \{\mathbf{M}, \mathbf{0}, \mathbf{0}\}, \quad (9)$$

where $\delta\omega = \omega - \omega^c$ and matrixes

$$\mathbf{A}_1 = \begin{bmatrix} \mathbf{A}^\circ & \mathbf{0} \\ \mathbf{0} & \mathbf{I}_{2n_q} \end{bmatrix}; \mathbf{B}_1 = \begin{bmatrix} \mathbf{0} & \mathbf{0} \\ \mathbf{0} & \mathbf{B}^\circ \end{bmatrix}; \mathbf{B}^\circ = \begin{bmatrix} -\mathbf{D} & -\mathbf{W} \\ \mathbf{I}_{2n_q} & \mathbf{0} \end{bmatrix}.$$

For calculation of the SC transfer functions, the system (9) is presented in the standard form of linear control system $\dot{\mathbf{x}} = \mathbf{A}\mathbf{x} + \mathbf{B}\mathbf{u}$; $\mathbf{y} = \mathbf{C}\mathbf{x}$, where for this case $\mathbf{x} = \{\delta\omega, \dot{\mathbf{q}}, \mathbf{q}\}$, $\mathbf{u} = \mathbf{M}$, and matrixes $\mathbf{A} = \mathbf{A}_1^{-1}\mathbf{B}_1$; $\mathbf{B} = \mathbf{A}_1^{-1}\{\mathbf{I}_3, \mathbf{0}, \mathbf{0}\}$ and $\mathbf{C} = \{\mathbf{I}_3, \mathbf{0}, \mathbf{0}\}$. The logarithmic frequency characteristics of continuous system from an input u_i to an output y_i , $i = x, y, z$ were obtained by specialized software. For multiple continuous-discrete ACS taking into account the different delays both a discrete measurement of the state vector and a physical forming the WPM control original methods (Somov, 2001) were applied (Somov, 2005b; Somov, 2005a). As an example, the logarithmic amplitude frequency characteristics subject to an absolute pseudo-frequency $\lambda = (2/T_u)\text{tg}(\omega T_u/2)$ on the Sesat open-loop pitch channel is presented in fig. 6 with $c_{z0}^\omega = 713.385$ s²/rad.

At mode of the SC guidance on the Sun we have vector $\mathbf{H} = \mathbf{0}$ and the SC searching motion is fulfilled with respect to the BRF axis Oy , e.g. vector

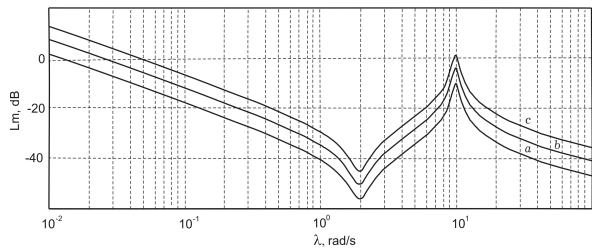


Figure 6. The logarithmic amplitude frequency characteristics on Sesat open-loop pitch channel: $a - c_z^\omega = c_{z0}^\omega$; $b - c_z^\omega = 2c_{z0}^\omega$; $c - c_z^\omega = 4c_{z0}^\omega$.

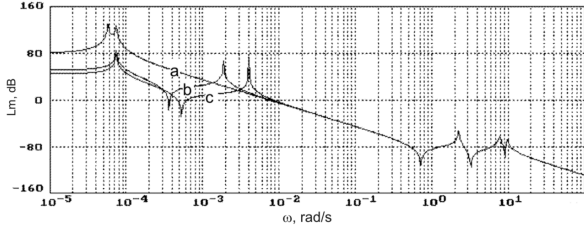


Figure 7. The logarithmic frequency characteristics of continuous pitch channel: a) $H=0$; b) $H=40$ Nms; c) $H=85$ Nms.

$\omega = \{0, \omega_y, 0\}$, for example $\omega_y = 0.2$ deg/s. Moreover the pitch and yaw channels have a weak gyroscopic connection which is essential only for the slowly motions. At mode of the Earth searching yet all three SC channels are gyromomently connected, but these influences are very weak. After finishing the Earth guidance mode the gyro stabilizer rotor begins to up-rotate and its own angular momentum H is increased up to value $H = 85$ Nms. Fig. 7 presents the SC logarithmic frequency characteristics of continuous pitch channel for three H values. Moreover it is appeared additional resonance peak by a nutation motion which is consistently changed to the right with increasing H as a parameter.

6 Nonlinear stability analysis of channels

The Lyapunov function method was used for a nonlinear stability analysis (Somov, 2005a). At simplest example, in a single-axis damping mode for the WPM parameters $T^d = 0$, $T_{zu}^d = 0$, $\tau_m = 0$, $\tau^m = T_u$, with an idealized measurement of angular rate and for its variation $\delta\omega_k \equiv \omega_k - \omega^c \equiv x_k$, the nonlinear channel discrete model is presented by the difference equation $x_{k+1} = x_k - b_d \text{Sat}(T_u, v_k)$; $v_k = k^\omega x_k$, where $b_d \equiv d_J = M^m/J$, k^ω and maximum torque M^m are parameters. For Lyapunov function $v_k \equiv v(x_k) = |x_k|$ there is derived the inequality $v_{k+1} = |x_k - b_d \text{Sat}(T_u, k^\omega x_k)| \leq |1 - b_d k^\omega| v_k$ for $x_k \neq 0$, moreover $v(0) = 0$. In result the rigorous condition for asymptotic stability of solution $x_k=0$ by this nonlinear model have the form $0 < b_d k^\omega < 2$, i.e. $0 < k^\omega < 2/b_d$.

In a single-axis attitude stabilization mode for same the PWM parameters and the state vector $\mathbf{x}_k \equiv \{\delta\alpha_k, \delta\omega_k\}$, the nonlinear channel model have the form

$$\begin{aligned} \mathbf{x}_{k+1} &= \mathbf{A}_d \mathbf{x}_k + (\mathbf{b}_d + \delta \mathbf{b}_d(\tau_k)) \text{Sat}(T_u, v_k^d); \\ v_k^d &= \mathbf{K}_d \mathbf{x}_k; \quad \tau_k = \text{Sat}(T_u, |v_k^d|); \\ \mathbf{A}_d &= \begin{bmatrix} 1 & T_u \\ 0 & 1 \end{bmatrix}; \quad \mathbf{b}_d = -d_J \begin{bmatrix} T_u \\ 1 \end{bmatrix}; \\ \delta \mathbf{b}_d(\tau_k) &= d_J \begin{bmatrix} \tau_k/2 \\ 0 \end{bmatrix}; \quad \mathbf{K}_d = [k^\alpha \quad k^\omega]. \end{aligned} \quad (10)$$

Let be $\mu \equiv 1 - d_J k^\omega$; $\chi \equiv k^\omega + k^\alpha T_u$; $\mu C_\theta \equiv 1 - d_J \chi/2$ and $\mu S_\theta \equiv d_J (4k^\alpha T_u/d_J - \chi^2)^{1/2}/2$ for the conditions $0 < \mu < 1$ and $\chi < 2(k^\alpha T_u/d_J)^{1/2}$. Then

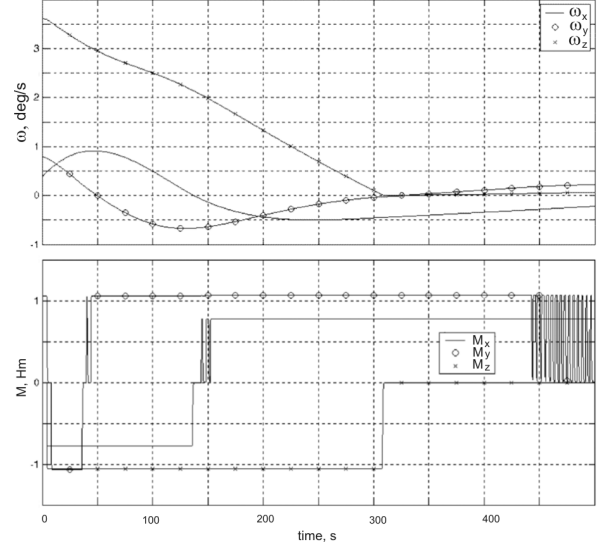


Figure 8. The SC body angular rates and the OEU control torques.

nonlinear model (10) stability is proved by Lyapunov function $v_k \equiv v(\mathbf{x}_k) = (\mathbf{x}_k^t \mathbf{V} \mathbf{x}_k)^{1/2}$ with matrix

$$\mathbf{V} \equiv (\mathbf{T}^t \mathbf{T})^{-1}; \quad \mathbf{T} \equiv \begin{bmatrix} T_u \mu C_\theta & T_u \mu S_\theta \\ \mu C_\theta - 1 & \mu S_\theta \end{bmatrix},$$

where matrix \mathbf{T} composed by eigenvectors of matrix $\mathbf{A}_d^o \equiv \mathbf{A}_d + \mathbf{b}_d \mathbf{K}_d$ for its eigenvalues $z_{1,2} = \mu(C_\theta \pm j S_\theta)$, $j \equiv \sqrt{-1}$. For this Lyapunov function there is derived the inequality $v_{k+1} \leq (\mu^2 + a v_k + b v_k^2)^{1/2} v_k$, where constant parameters $a > 0$ and $b > 0$ are appeared during a majorizing procedure. That inequality is the basis for obtaining the rigorous conditions of asymptotic stability of solution $\mathbf{x}_k = \mathbf{0}$ by nonlinear discrete channel model and also for estimating its guaranteed attracting set by the inequality $\mathbf{x}_0^t \mathbf{V} \mathbf{x}_0 \leq (a^2 - 4b(\mu^2 - 1))/(4b^2)$.

7 Parametric synthesis and analysis by imitation

Detailed nonlinear dynamical analysis of the flexible spacecraft ACS and parametric synthesis of discrete control laws on channels were carried out by methods of computer simulation which were realized at Matlab environment (Butyrin and Somov, 2004). In the initial damping mode for various initial conditions on coordinates on the SAPs' oscillation tones analysis of the SC dynamics was carried out. For example, at given initial conditions $\mathbf{q}_1(0) \equiv \{q_{11}, q_{12}, q_{13}\} = \{0.2, -0.3, -0.2\}$; $\dot{\mathbf{q}}_1(0) = \mathbf{0}$; $\mathbf{q}_2(0) \equiv \{q_{21}, q_{22}, q_{23}\} = \{-0.2, 0.3, 0.1\}$; $\dot{\mathbf{q}}_2(0) = \mathbf{0}$ numerical results are presented in fig. 8 – fig. 10.

At the SC guidance on the Sun and on the Earth by elaborated discrete control laws for a width-pulse modulation of the jet engine thrust, the SC structure flexibility have smaller influence at comparison with the initial damping mode yet for decrement $\delta = 10^{-3}$ of oscillations.

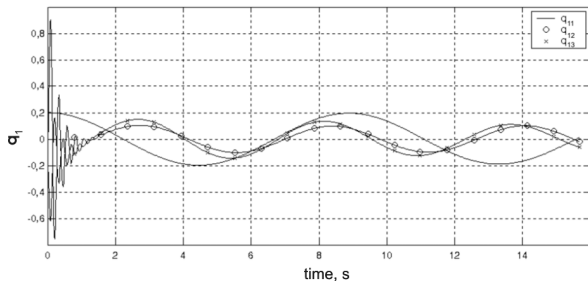


Figure 9. Oscillations of 1-st wing on 1-st three tones.

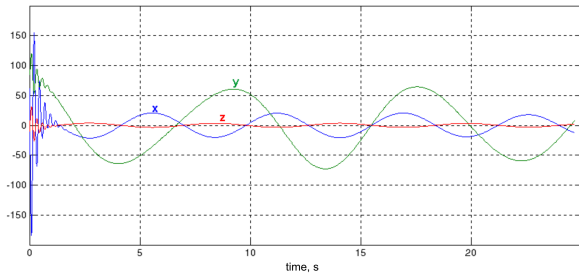


Figure 10. Deviations of 1-st wing's point #1 on fig. 3 in mm from its equilibrium position.

8 The flexible SC motion animation

Russian software environment *Super Vision* (the NPO PM development) was applied for animation of the SC motion with flexible active SAPs. In used version of this software the requirement specification is applied for creation and tuning the reflected objects. Interface between components of the elaborated software for simulation and visualization of the SC flexible structure motion is carried out by files on hard disk. In stage 1 the SC damping mode simulation is fulfilled. In the Matlab environment the Simulink is started, results of the subsystem work are graphics of the transient processes on the ACS state coordinates and the data files, which are recorded on hard disk. In stage 2 the data preparation is carried out for animation of the SC body motion and the flexible SAPs' oscillations by applied visualization system. At loading the file `panel.svn` there will be reflected the indicated SAPs' wing oscillations, and if file `mnk.svn` is loaded – the SC body motion in the ORF. Some results obtained by the elaborated software are presented in fig. 11.

9 Conclusion

Problems of nonlinear modeling, dynamic synthesis and analysis, simulation and visualization of a flexible spacecraft spatial motion were considered. The obtained results on a multiple filtering and a width-pulse control for the communication satellite with large-scale solar array panels were represented.

Acknowledgements

The work was supported by the RAS Presidium (Pr. 22), the Division on EMMCP of RAS (Pr. 15) and the RFBR (07-08-97611, 08-08-00512, 08-08-99101).

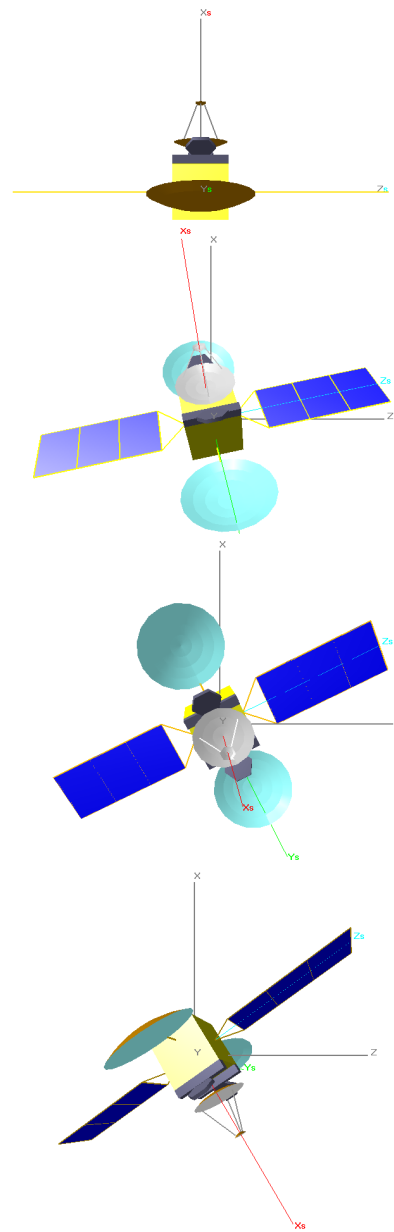


Figure 11. The animation frames of the SC attitude motion.

References

- Butyrin, S.A. and S.Ye. Somov (2004). Modeling a flexible structure motion of the *sesat* satellite. In: *Proceedings of II All-Russian scientific conference "Designing Scientific and Engineering Application in the Matlab environment"*. Vol. 2. ICS of RAS. Moscow. pp. 101–121.
- Somov, S.Ye. (2005a). A damping dynamics of a flexible satellite at a width-pulse modulation control of engines. *Avatsionnaya Tekhnika* (4), 17–23.
- Somov, S.Ye. (2005b). Nonlinear dynamics of a flexible satellite at initial damping. *Izvestiya of Samara Scientific Center of RAS* 7(1), 107–117.
- Somov, Ye.I. (2001). Robust stabilization of a flexible spacecraft at partial discrete measurement and a delay in forming control. *Journal of Computer and Systems Sciences International* 40(2), 287–307.